

# Soft Matter

Accepted Manuscript



This is an *Accepted Manuscript*, which has been through the Royal Society of Chemistry peer review process and has been accepted for publication.

*Accepted Manuscripts* are published online shortly after acceptance, before technical editing, formatting and proof reading. Using this free service, authors can make their results available to the community, in citable form, before we publish the edited article. We will replace this *Accepted Manuscript* with the edited and formatted *Advance Article* as soon as it is available.

You can find more information about *Accepted Manuscripts* in the [Information for Authors](#).

Please note that technical editing may introduce minor changes to the text and/or graphics, which may alter content. The journal's standard [Terms & Conditions](#) and the [Ethical guidelines](#) still apply. In no event shall the Royal Society of Chemistry be held responsible for any errors or omissions in this *Accepted Manuscript* or any consequences arising from the use of any information it contains.



## Modulation of Partition and Localization of Perfume Molecules in Sodium Dodecyl Sulfate Micelles

Yaxun Fan,<sup>a</sup> Haiqiu Tang,<sup>\*b</sup> Ross Strand,<sup>b</sup> and Yilin Wang<sup>\*a</sup>

Received 00th January 2015,  
Accepted 00th January 2015

DOI: 10.1039/x0xx00000x

[www.rsc.org/softmatter](http://www.rsc.org/softmatter)

Influence of perfume molecules on the self-assembly of anionic surfactant sodium dodecyl sulfate (SDS) and their localization in SDS micelles have been investigated by  $\zeta$  potential, small angle X-ray scattering (SAXS), one- and two-dimensional NMR and isothermal titration microcalorimetry (ITC). A broad range of perfume molecules varying in octanol/water partition coefficients  $P$  are employed. The results indicate that the surface charge, size and aggregation number of the SDS micelles strongly depend on the hydrophobicity/hydrophilicity degree of perfume molecules. Three distinct regions along the  $\log P$  values are identified. Hydrophilic perfumes ( $\log P < 2.0$ ) partially incorporate into the SDS micelles and do not lead to micelle swelling, whereas hydrophobic perfumes ( $\log P > 3.5$ ) are solubilized close to the end of the hydrophobic chains in the SDS micelles and enlarge the micelles with higher  $\zeta$  potential and larger aggregation number. The incorporated fraction and micelle properties show increasing tendency for the perfumes in the intermediate  $\log P$  region ( $2.0 < \log P < 3.5$ ). Besides, the molecular conformation of perfume molecules also affects these properties. The perfumes with linear chain structure or aromatic group can penetrate into the palisade layer and closely pack with the SDS molecules. Furthermore, the thermodynamic parameters obtained from ITC show that the binding of the perfumes in intermediate  $\log P$  region is more spontaneous than those in the other two  $\log P$  regions, and the micellization of SDS with the perfumes is driven by entropy.

### Introduction

Perfumes are very important ingredients in home and personal care products, or even beverages.<sup>1,2</sup> It was generally assumed that a small amount of perfume had little effect on the formulation of these water-based consumer products. Actually, the perfume molecules can give rise to a great range of interactions with surfactants, and alter the phase behaviour of surfactant-based systems and formulation stability.<sup>3,4</sup> So far, a wide range of different perfume molecules have discovered and synthesized, such as alcohols, phenols, esters and lactones,<sup>5</sup> which are likely to result in diversity in their effects on surfactant self-assembly. Their relative hydrophilicity/hydrophobicity is often used as classify criterion, and approximately characterized by the ratio of the concentrations of perfumes in octanol and water in equilibrium, i.e.,  $\log P$ .

The interaction between surfactants and perfumes has been studied from various aspects. One of the main methods used to study the interaction of surfactants with perfumes is evaporation measurement.<sup>6-11</sup> Behan et al.<sup>6</sup> found headspace concentrations of

benzyl acetate above the surfactant solutions were directly proportional to the phase volume ratio, and in turn could be rationalized in terms of a simple partition model. Friberg et al.<sup>7,8</sup> measured the vapour pressure of perfumes by gas chromatographic analysis of headspace vapour at equilibrium, and studied the surfactant phase behaviour in the perfume emulsions during the evaporation process. They concluded that more hydrophilic phenylethanol and benzaldehyde were located in aqueous headgroup regions, and more hydrophobic limonene was located in hydrophobic regions of a lamellar phase. Combining headspace solid-phase microextraction (HS-SPME) with GC/MS is a convenient and effective method for quantifying the equilibrium partitioning of a perfume compound between water and surfactant micelles. The concentration of a perfume in headspace as a function of surfactant concentration is used to fit a mass balance, achieving the partition coefficient of the perfume and the critical micelle concentration of the surfactant. By this method, Lloyd et al.<sup>9</sup> found when the concentration of limonene in the SDS/limonene system was low enough that it could be completely dissolved by water in the absence of micelles, then a constant value for the partition coefficient was obtained, independent of the limonene concentration. However, at high total limonene concentration, the partition coefficient became a function of the amount of limonene in micelles.

The impacts of perfumes on surfactant self-assembly have also been extensively studied from the perspective of perfume solubilization.<sup>12-15</sup> Abe et al.<sup>12-14</sup> systematically investigated the solubilization of a range of synthetic perfumes in mixed anionic-

<sup>a</sup> Key Laboratory of Colloid and Interface Science, Beijing National Laboratory for Molecular Sciences (BNLMS), Institute of Chemistry, Chinese Academy of Sciences, Beijing 100190, P. R. China, E-mail: yilinwang@iccas.ac.cn.

<sup>b</sup> Procter & Gamble Technology (Beijing) Co. Ltd, Beijing 101312, P. R. China. E-mail: tang.ha@pg.com

<sup>†</sup> Electronic Supplementary Information (ESI) available: Calculation of the fraction of perfume molecules incorporated into micelles and the analysis data from SAXS. See DOI: 10.1039/x0xx00000x

nonionic surfactant solutions by measuring maximum additive concentration and determining the distribution coefficient between micellar and bulk phases. The negative synergistic effect on the distribution coefficient values of perfumes became greater when the perfume was more hydrophobic and the nonionic surfactant had shorter EO chains. Based on many experimental solubilization data, the thermodynamic theory of solubilization was developed by Nagarajan,<sup>15</sup> improving quantitative understanding of the solubilization phenomenon. The thermodynamic studies used assumptions about the structure of the aggregates in order to simplify the estimation of thermodynamic variables. In this case, the real aggregate structures where perfumes are solubilized are still desired to improve the thermodynamic understanding.

Further understanding about the aggregate structures and the interaction in surfactant/perfume mixtures has been achieved by investigating the localization of perfume molecules in surfactant micelles,<sup>16-25</sup> and by obtaining more precise size or shape of surfactant/perfume aggregates.<sup>20-22</sup> Mahapatra<sup>16</sup> and Fischer et al.<sup>17</sup> pursued the partition and localization of different perfume molecules in surfactant micelles by <sup>1</sup>H NMR and Pulsed Field Gradient (PFG)-NMR. A series of perfume molecules possessing a wide variety of functional groups with different degrees of hydrophilic/hydrophobic character were employed. They confirmed and expanded the conclusions obtained by Friberg et al.<sup>8</sup> mentioned above, and proposed more detailed descriptions about the localization of perfume molecules. Hydrophilic perfumes locate at micelle-water interface, the hydrophobic ones reside in the core of micelles, while only perfumes with intermediate log*P* values insert in the palisade layer of micelles, promoting micellar growth. Lindman et al.<sup>18</sup> studied the solubilization of three perfumes differing in polarity in hexagonal liquid crystal of triblock copolymer using small-angle X-ray scattering. Through calculating the interfacial area per polyethylene oxide block and the radius of the apolar domain, the similar location trends of each perfume in the association structure were determined. Thomas and co-workers<sup>20-22</sup> obtained detailed structural information about the impact of the different perfume molecules on surfactant self-assembly in bulk and at air-water interface by small-angle neutron scattering and neutron reflectivity. The properties of perfumes, including structure, solubility and degree of hydrophilicity/hydrophobicity, were correlated with the self-assembling structures of surfactants.

In the present work, effects of a broad variety of perfume molecules on surfactant self-assembly have been investigated.  $\zeta$  potential and SAXS are used to provide the structural information of surfactant aggregates, one- and two-dimensional NMR are applied to obtain the detailed information of surfactant/perfume interaction in molecular level, and isothermal titration microcalorimetry (ITC) is used to determine thermodynamic parameters of surfactant/perfume interactions. Our goal is to relate the differences in the aggregation behaviour of surfactant to the molecular structures of perfumes, and improve the understanding of the effect of perfume molecules on surfactant self-assembly. Anionic surfactant sodium dodecyl sulfate (SDS) was chosen as a representative of anionic surfactants, which has been extensively used to build the basic formulation of a variety of home and personal care products.<sup>26-28</sup> The perfumes chosen cover a very broad range of molecular structures and the log*P* values change

from 0.27 to 4.46. Methyl Paraben as a preservative is also studied here because it has the similar molecular structure to perfumes and is an important ingredient in personal care products. In the following sections, the results about Methyl Paraben are discussed in perfume molecules without using a separating category. The chemical structures, molecular weight and log*P* values of perfume molecules are shown in Table 1.

**Table 1.** Chemical structures, molecular weight and log*P* values of perfume molecules.

Perfume Molecule	Chemical Structure	Molecular Weight	log <i>P</i>
Pinene (PN)		136.24	4.46
Limonene (LM)		136.24	4.38
Menthyl Acetate (MA)		198.30	3.78
Eucalyptol (EP)		154.25	3.15
Menthol (ML)		156.27	3.06
Menthone (ME)		154.25	3.05
Piperitone (PT)		152.23	2.76
Carvone (CV)		150.22	2.47
Linalool (LL)		154.25	2.44
Anethole (AT)		148.20	2.43
Methyl Salicylate (MS)		152.15	2.08
Methyl Paraben (MP)		152.15	1.70
Ethyl Butyrate (EB)		116.16	1.41
Ethyl Acetate (EA)		88.11	0.27

## Experimental

### Materials

SDS (>99%) was purchased from Sigma-Aldrich. 14 model perfumes with high purity (>98%) were used without further purification. The log*P* values of the perfume molecules were determined by High Performance Liquid Chromatography (HPLC). The Milli-Q water (18 M $\Omega$ -cm) was used in all experiments.

### Preparation of SDS/Perfume Solutions

SDS was dissolved in deuterium oxide (D<sub>2</sub>O)/H<sub>2</sub>O mixture (5.0 w % D<sub>2</sub>O, CIL Cambridge Isotope Laboratories, purity>99.9%) to prepare a basic stock solution of 97.5 mM SDS solution. The SDS/perfume

mixed solutions were prepared by adding 0.3 wt% perfumes at 25 °C. Homogeneous and stable SDS/perfume solutions were obtained with a fixed perfume content of 0.3 wt% for all the following measurements.

### ζ Potential Measurements

ζ potential measurements of the SDS/perfume solutions were performed by a Malvern Zetasizer Nano-ZS instrument (ZEN3600, Malvern Instruments, Worcestershire, UK) equipped with a 4 mW He-Ne laser at a wavelength of 633 nm. The samples were equilibrated for 2 min inside the instrument before dynamic light backscattering (detection angle = 173°) at 25.0 °C. The ζ potentials were calculated from the mobility measured in electrophoretic light-scattering (ELS) mode:  $\mu_0 = 2\epsilon\zeta f(\kappa a)/3\eta$ , where  $\epsilon$  and  $\eta$  are taken as the dielectric constant and viscosity of pure water, respectively, and  $f(\kappa a)$  is the Henry's function wherein  $\kappa$  is the Debye-Hückel parameter and  $a$  is the particle (micelle) radius.

### Small Angle X-ray Scattering (SAXS)

SAXS experiments were performed in situ at BL16B1 beamline in Shanghai Synchrotron Radiation Facility (SSRF) with the radiation wavelength  $\lambda = 1.24 \text{ \AA}$ .<sup>29</sup> In experiments, the sample-to-detector distance was 1914.5 mm. For SAXS data collection, a Mar165 CCD detector with an average pixel size of  $80 \times 80 \mu\text{m}^2$  was used. The experiments were carried out at room temperature (25 °C) under condition of 8 keV photon energy and 300 nm small-angle resolutions. All SAXS patterns were first radially averaged to obtain the intensity  $I(q)$  ( $q = 4\pi / \sin\theta$ ) and then corrected for background scattering and X-ray absorption. The 2D SAXS scattering patterns were analyzed using Fit2D software. The synchrotron SAXS patterns were normalized using the primary beam intensity and corrected for background scattering of solvent. The normalized data was fitted by using SasView<sup>30</sup> with the Ellipsoid model. The model yields the radius along the rotation axis of the ellipsoid  $R_a$ , and the radius perpendicular to the rotation axis  $R_b$ . The radius of gyration ( $R_g$ ) of the ellipsoid is then calculated with the equation  $R_g = ((R_a^2 + R_b^2)/4)^{1/2}$ . The aggregation number ( $N_{\text{agg}}$ ) was approximately calculated on the basis of the volume of the ellipsoidal micelles ( $V_{\text{ellipsoid}} = 4\pi/3 \times R_a \times R_b^2$ ), and the molecular volume of the SDS monomers ( $4.8 \times 10^3 \text{ \AA}^3$ ).<sup>31</sup>

### Nuclear Magnetic Resonance (NMR)

<sup>1</sup>H NMR, DOSY and NOESY experiments were all performed on a Bruker Avance 600 spectrometer at 25 °C. The center of the HDO signal (4.79 ppm) was used as the reference in the D<sub>2</sub>O/H<sub>2</sub>O solutions. In all the NMR experiments, the number of scans was 32 to achieve good signal-to-noise ratios, and was recorded with a digital resolution of 0.04 Hz/data point. DOSY spectra were obtained with the stebppp1s pulse program and a maximum gradient strength of 50 G·cm<sup>-1</sup>. The gradient field was linearly increased in 32 steps, resulting in an attenuation of <sup>1</sup>H NMR from 2% to 95%. The NOESY experiments were carried out with the standard three-pulse sequence with a mixing time of 800 ms.

### Isothermal Titration Microcalorimetry (ITC)

ITC measurements were taken on a TAM2277-201 microcalorimeter (Thermometric AB, Järfälla, Sweden) with a stainless steel sample cell of 1 ml at 25.00 °C. The sample cell of the microcalorimeter was

initially loaded with 800 μl of 0.3 wt% perfume in D<sub>2</sub>O/H<sub>2</sub>O. 200 mM SDS solution was injected consecutively into the stirred sample cell using a 500 μl Hamilton syringe controlled by a Thermometric 612 Lund pump until the desired concentration range had been covered. During the whole titration process, the system was stirred at 90 rpm with a gold propeller, and the interval between two injections was long enough for the signal to return to the baseline. The observed enthalpy ( $\Delta H_{\text{obs}}$ ) was obtained by integrating the areas of the peaks in the plot of thermal power against time.

## Results and discussion

### Effects of Perfumes on SDS Micelles

Fig. 1 shows the ζ potential values for the SDS/perfume mixture with different log*P* values, fixing the concentrations of SDS and perfume at 97.5 mM and 0.3 wt%, respectively. All the SDS/perfume mixtures with the perfumes of different log*P* values are transparent and homogeneous at 25 °C. Although all the perfumes studied are uncharged, the ζ potential values of the mixtures change obviously. In the absence of perfumes, the ζ potential of the SDS micelles is about -20±4 mV. With the addition of perfumes, the ζ potential values are relevant with the log*P* values of perfumes, and display three distinct regions with the increase of the log*P* value. The ζ potential values of SDS/perfume mixed micelles are almost unchanged when log*P* < 2.0, whereas a steep increase occurs when the log*P* is beyond 3.5. During the intermediate log*P* region of 2.0 < log*P* < 3.5, the variation of the ζ potential values is between the above two situations. Because the perfumes are all non-ionic, the results indicate that the perfumes with a larger log*P* value make the charged SDS molecules pack more tightly in micelles.

To assess structural details of the SDS/perfume mixed micelles, SAXS measurements were performed on the same samples. Characteristic scattered intensities  $I(q)$  versus scattering vector  $q$  are shown in Fig. 2a. All scattering curves present a broad peak at  $q \approx 1.7 \text{ nm}^{-1}$ , which is characteristic of the intramicellar form factor.<sup>32,33</sup> Obviously, this peak changes by adding different perfumes, indicating that the SDS micelles are dramatically affected by the properties of these perfumes. The presence of a second peak at  $q \approx 0.6 \text{ nm}^{-1}$  is a fingerprint of structure factor affected by the interaction between charged SDS micelles. In general, concentration effects become visible at small angles by the formation of an additional peak and the descent in intensity in this region is typical for repulsive interaction potentials. Herein the SDS or SDS/perfume solutions are concentrated and the micelles are strongly charged, resulting in the strong influence of structure factor in the small  $q$ -values. The satisfactory fits of SAXS curves for the different SDS/perfume systems were obtained while applying SasView software by the Ellipsoid model. The structural parameters of the SDS and SDS/perfume micelles from the SAXS data fitted with the ellipsoid model, including the radius along the rotation axis of the ellipsoid  $R_a$ , the radius perpendicular to the rotation axis  $R_b$ , the radius of gyration ( $R_g$ ), and the aggregation number ( $N_{\text{agg}}$ ), are derived and summarized in Table S1 of Supporting Information. These parameters are plotted against log*P* in Fig. 2b and Fig. 2c. The structural parameters for the SDS micelles without perfumes are

consistent with those in literature,<sup>31,34</sup> and indicate that the concentrated SDS micelles are in an ellipsoidal shape. With the addition of perfumes, the SDS/perfume mixed micelles still keep ellipsoidal shape, but all the values of  $R_a$ ,  $R_b$ ,  $R_g$  and  $N_{agg}$  increase with the increase of  $\log P$ . Obviously, the aggregation number and the size of the SDS/perfume micelles almost increase with the increase of the  $\log P$  values, which is similar to the changing tendency of  $\zeta$ -potential. It suggests that the addition of more hydrophobic perfumes induces the larger mixed micelles with higher  $\zeta$ -potential and larger aggregation number.

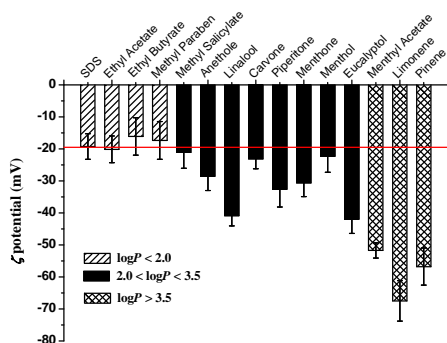


**Fig. 1.**  $\zeta$  potential values of SDS micelles and SDS/perfume mixed micelles with different  $\log P$  values at 25.0 °C. The red line reflects the  $\zeta$  potential of SDS micelles without perfumes.

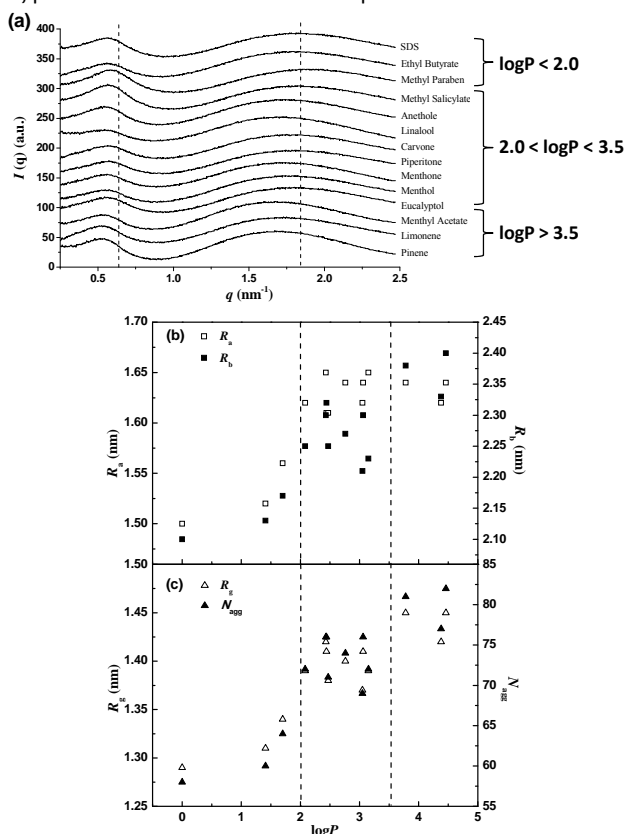


**Fig. 2.** (a) SAXS curves for pure SDS solution and SDS/perfume micelle solutions with different  $\log P$  values at 25 °C. (b) The semiaxes of the ellipsoids  $R_a$  and  $R_b$  obtained by fitting the SAXS curves, and (c) the radius of gyration ( $R_g$ ) and aggregation number ( $N_{agg}$ ) of the ellipsoidal micelles for pure SDS micelles and SDS/perfume mixed micelles.

In brief, the hydrophilicity/hydrophobicity of perfumes is crucial to the influences on the size and charge density of the SDS/perfume mixed micelles. When the perfumes are very hydrophilic ( $\log P < 2.0$ ), they do not affect the micelles. While the perfumes are very hydrophobic ( $\log P > 3.5$ ), the perfumes pronouncedly lead to the swelling of the SDS micelles and the more densely packing of SDS molecules. As the hydrophilicity/hydrophobicity of perfumes is intermediate ( $2.0 < \log P < 3.5$ ), their impacts on the SDS micelles are also basically between the above two cases, but not completely consistent, which will be discussed in the later text. These results mean that the hydrophilicity/hydrophobicity of perfumes affects their interaction with micelles and their incorporation in micelles.

### Partition and Localization of Perfumes in SDS Micelles

In order to understand the interaction of perfumes with SDS micelles and the incorporation of perfumes in SDS micelles, several NMR techniques including  $^1\text{H}$  NMR spectra, DOSY and 2D NOESY have been applied. The variations of proton-chemical shifts for SDS induced by adding the same amount of perfumes with different  $\log P$  values are shown in Fig. 3. Starting from the hydrophilic headgroup, SDS exhibits four types of protons in its  $^1\text{H}$  NMR spectrum, including  $\alpha$ - and  $\beta$ -methylene ( $\text{H}_c$  and  $\text{H}_d$ ), nine bulk methylene ( $\text{H}_b$ ), and the terminal methyl protons ( $\text{H}_a$ ). A minimum quantity 0.3 wt% of perfume turns out to be sufficient to obtain sufficiently intensive  $^1\text{H}$  signals for perfume molecules, which are spectrally resolved and well discriminated from the  $^1\text{H}$  signals of SDS. As shown in Fig. 3, all  $\text{H}_a$  and  $\text{H}_b$  of SDS shift upfield in the presence of perfume molecules, and the changing extents are dependent on the hydrophilic/hydrophobic properties of the perfume molecules. However,  $\text{H}_c$  and  $\text{H}_d$ , which are closely linked to the charged sulfate groups, exhibit larger upfield shifts with the perfumes in the intermediate  $\log P$  region, but less upfield shifts with the perfumes in low or high  $\log P$  region. The results mean that all the perfume molecules incorporate into the SDS micelles, but the localizations of perfume molecules are different. When  $\log P < 2.0$ , the perfume molecules may be located in the headgroup regions of SDS micelles, where  $\alpha$ - and  $\beta$ -methylene protons ( $\text{H}_c$  and  $\text{H}_d$ ) become shielded and thus the chemical shifts move upfield, while the other methylene ( $\text{H}_b$ ) and terminal methyl protons ( $\text{H}_a$ ) or the SDS chains almost do not change. When  $2.0 < \log P < 3.5$ , more perfume molecules may penetrate into the palisade layer of the SDS micelles, leading to the chemical shifts of all the protons in the hydrophobic chains move upfield. When  $\log P > 3.5$ , terminal methyl protons ( $\text{H}_a$ ) of SDS rather than the  $\alpha$ -methylene protons ( $\text{H}_d$ ) move upfield, which indicates that the perfume molecules may be located near the hydrophobic cores of the SDS micelles.

Furthermore, DOSY was performed on the SDS/perfume micellar solutions. Self-diffusion coefficients obtained are plotted against  $\log P$  of the perfumes in Fig. 4. For free perfumes without SDS, the diffusion coefficients are in the order of  $D = 1 \times 10^{-9} \text{ m}^2/\text{s}$ . In the SDS micelles, the diffusion coefficient of perfumes decreases significantly, which can be attributed to the association of perfumes with SDS micelles. In the case with low  $\log P$  values, the perfume diffusion coefficients are reduced by about a factor of 2 compared to the values of free perfumes. From 2.0 to 2.5 of  $\log P$ , the diffusion coefficient decreases obviously and almost reaches the diffusion coefficient of the SDS micelle itself. When  $\log P$  is beyond 2.5, the

diffusion coefficient does not change anymore. These results prove that the perfume molecules are incorporated into the micelles and the degree of incorporation increases with increasing  $\log P$ . On the other hand, the diffusion coefficient of SDS is also closely related with the  $\log P$  value of the added perfumes. The diffusion coefficient of SDS starts to decrease around  $\log P = 1.5$  and become the lowest value at high  $\log P$  values ( $\log P > 3.5$ ). The decrease of the SDS diffusion coefficient is caused by the size increase of the SDS micelles upon the incorporation of the perfumes and the incorporation is gradually enhanced by the increasing hydrophobicity of the perfumes. At  $\log P > 3.5$ , the perfumes completely locate in the hydrophobic core of SDS micelles, resulting in the lowest diffusion coefficient of SDS. The varying trend is in good agreement with the  $\zeta$  potential and SAXS results mentioned above.

These results can also be interpreted by calculating the fraction of the perfume molecules incorporated in SDS micelles. Based on the assumptions and equations described in Supplementary Information, the values of the fractions of perfumes incorporated in micelles,  $f_p$ , are extracted from the respective diffusion coefficients  $D$ , diffusion coefficient of free perfume molecules ( $D_f$ ) and the diffusion coefficient of SDS in the SDS/perfume micelles ( $D_M$ ). As shown in Fig. 5, with a  $\log P$  smaller than 2.0, 80-85% perfume molecules are incorporated into the SDS micelles, while the remaining perfume molecules diffuse freely in aqueous phase. Between 2.0 and 3.5 of  $\log P$ , it is a transition region of increasing perfume content incorporated in micelles. Above  $\log P > 3.5$ , almost all the perfume molecules are incorporated in the micelles. This result is consistent with the expectation relying on the increase of perfume hydrophobicity.

In order to further understand the microstructure of the SDS/perfume micelles, 2D NOESY experiments have also been applied to obtain more direct and effective information about the group relationship in the SDS and perfume molecules. Generally, the appearance of a NOE cross-peak between two nuclei in a sufficiently short mixing time implies that the protons are within a distance of 5 Å, indicating that these protons closely interact with each other. Although it is difficult to calculate the exact distance between the SDS and perfume molecules, the NOE signals do exist originated from the intermolecular interactions between the SDS and perfume molecules. Table 2 summarizes the internuclear NOEs observed between SDS and the perfumes.

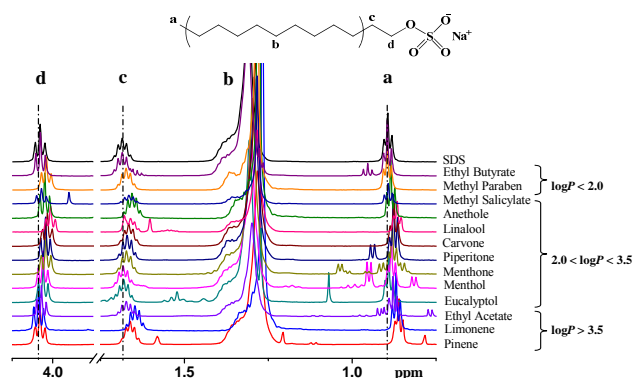


Fig. 3.  $^1\text{H}$  NMR spectra of pure SDS and SDS/perfume micellar solutions with different  $\log P$  values.

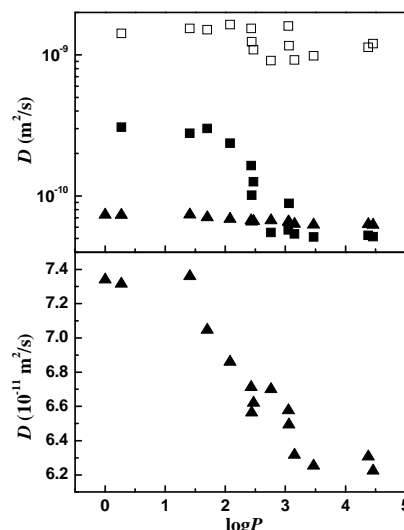


Fig. 4. Self-diffusion coefficients as a function of  $\log P$  of the perfumes: perfumes in  $\text{D}_2\text{O}$  ( $\square$ ); perfume molecules ( $\blacksquare$ ) and SDS ( $\blacktriangle$ ) in SDS/perfume mixed micelles containing 0.3 wt% perfumes.

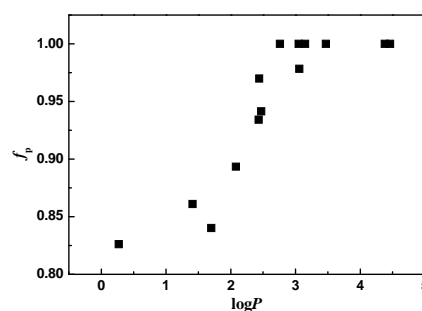


Fig. 5. The fraction of the perfumes incorporated in the SDS micelles against  $\log P$  of the perfumes.

Table 2. The spatially correlated relationship between protons of SDS and perfumes according to the NOESY results in the absence and presence of perfumes with different  $\log P$ .

$\log P < 2.0$		$2.0 < \log P < 3.5$		
Ethyl Butyrate	Methyl Paraben	Methyl Salicylate	Anethole	Linalool
$2.0 < \log P < 3.5$				
Carvone	Piperitone	Menthone	Menthol	Eucalyptol

When  $\log P < 2.0$ , NOEs are observed between the perfume molecules and the  $\alpha$ - and  $\beta$ -methylene in the hydrophobic chains of SDS, but no NOEs can be detected between the perfumes and the terminal methyl or the other nine bulk methylenes of SDS. So the perfumes with low  $\log P$  values are predominantly localized in the SDS micelles but close to the SDS headgroup. This situation almost does not alter the structures of SDS micelles.

When  $2.0 < \log P < 3.5$ , the NOEs between the perfumes and SDS do not follow a single interaction profile. For Methyl Salicylate, Carvone and Menthol, the NOE signals appear between the protons of the perfumes and the hydrophobic chain close to the headgroups of SDS, similar to the hydrophilic perfumes at  $\log P < 2.0$ . For Anethole, Linalool, Piperitone and Eucalyptol, the NOE signals exist between the perfumes and the whole hydrophobic chains of SDS, from  $\alpha$ -methylene to terminal methyl protons. As to Menthone, NOEs are observed between Menthone and the hydrophobic chains of SDS just near the micellar core. These phenomena indicate that other chemical structural factors of the perfumes besides the properties described by  $\log P$  also affect their incorporation in micelles. As observed above, Carvone has the similar  $\log P$  value to Linalool and Anethole, but their incorporation in the SDS micelles are different. Carvone molecules show a twisted conformation due to the cyclohexene group, Linalool has a linear structure, but Anethole has a rigid conjugated structure. Probably because of the favourable steric structure of Linalool and the strong cooperate interaction of Anethole, they may easily penetrate into the palisade layer and pack closely with the SDS molecules, in turn leading to the micelle growth. In addition, Menthone is solid in room temperature, so it tends to penetrate into the core of SDS micelles. The other four perfumes in the intermediate  $\log P$  region, Anethole, Linalool, Piperitone and Eucalyptol, incorporate in the palisade layers of the SDS micelles and efficiently reduce spontaneous curvature of micelles.

In the  $\log P$  region larger than 3.5, the NOE signals can hardly be detected between the perfumes and SDS. The obvious micellar growth, significantly enhanced micellar charge density, and large incorporated fraction of the perfumes in micelles have indicated that the perfumes in this region have been completely incorporated into the SDS micelles. The tight and deep packing of the perfumes in the micelles might make the NOE signals undetectable.

Reviewing the structure information of the SDS micelles in the presence of the perfumes (Fig. 2), it is noted that the perfumes located near the core of the micelles increase the size and aggregation number of the micelles more obviously, and basically the deeper the perfumes in micelles, the larger the micellar size and aggregation number.

### Interaction of Perfumes with SDS

ITC has been widely utilized to study intermolecular interactions in solution from thermodynamic aspect, such as drug-excipient interactions.<sup>35-37</sup> Herein ITC is used to study the interaction of the nonionic perfumes with SDS micelles. Fig.6 shows the changes of the observed enthalpy ( $\Delta H_{\text{obs}}$ ) against the final SDS concentration ( $C_{\text{SDS}}$ ) when SDS (200 mM) is titrated into the aqueous solution of perfume molecules (0.3 wt%). The titration curves of SDS are all approximately sigmoidal in shape and each can be subdivided into two concentration regions separated by a transition region

associated with micelle formation, corresponding to the critical micelle concentration (CMC) of SDS. When  $C_{\text{SDS}}$  is below CMC, all added SDS micelles are demicellized into monomers and the monomers are further diluted. When  $C_{\text{SDS}}$  is beyond CMC, only the micellar solution is diluted and finally  $\Delta H_{\text{obs}}$  drops toward zero. Comparing with the  $\Delta H_{\text{obs}}$  curves of SDS being titrated into water, the presence of the perfumes changes the CMC values and/or change the  $\Delta H_{\text{obs}}$  values in this process. The differences between the  $\Delta H_{\text{obs}}$  curve of SDS without perfumes and the  $\Delta H_{\text{obs}}$  curve of SDS with a perfume are ascribed to the interaction between SDS and the perfume. As illustrated in previous work,<sup>38</sup> the  $\Delta H_{\text{obs}}$  curves are fitted and differentiated with respect to  $C_{\text{SDS}}$ , then the position of the extremum is taken as the CMC and the values of  $\Delta H_{\text{mic}}$  are determined from the enthalpy difference between the two linear segments of the  $\Delta H_{\text{obs}}$  curves extrapolated to the CMC. The obtained CMC and  $\Delta H_{\text{mic}}$  values are expressed by per mole of SDS. Similar to the method used by Thomas et al.<sup>39</sup> and Wang et al.<sup>40</sup> in studying the interaction of surfactants with polymers, the following analysis is used to study the interaction of the perfumes with SDS. The free energy of micellization ( $\Delta G_{\text{mic}}$ ) of SDS in the absence and presence of perfumes can be calculated using the equation of  $\Delta G_{\text{mic}} = (1+K)RT[\text{CMC}]$ , where  $K$  is the effective micellar charge fraction, which can be obtained by extrapolating the slope of a plot of  $\ln[\text{CMC}]$  versus  $\ln[\text{counterion}]$ . For SDS,  $K$  was used as 0.85.<sup>41</sup> Once the values of  $\Delta G_{\text{mic}}$  and  $\Delta H_{\text{mic}}$  have been obtained, the entropy changes  $\Delta S_{\text{mic}}$  can be calculated by  $\Delta S_{\text{mic}} = (\Delta H_{\text{mic}} - \Delta G_{\text{mic}})/T$ . In assuming the SDS molecules without perfumes exist in a similar micellar environment as that with perfumes, the free energy of the SDS/perfume interaction ( $\Delta G_{\text{ps}}$ ) can be derived by subtracting the  $\Delta G_{\text{mic}}$  of SDS without perfumes from the  $\Delta G_{\text{mic}}$  of SDS with perfumes. The micellization of SDS without and with perfumes can be expressed as  $n\text{S} \rightarrow \text{S}_n$  ( $\Delta G_{\text{mic}}, 1$ ) and  $n\text{S} + m\text{P} \rightarrow \text{S}_n\text{P}_m$  ( $\Delta G_{\text{mic}}, 2$ ) respectively. If equation (2) minus equation (1),  $\text{S}_n + m\text{P} \rightarrow \text{S}_n\text{P}_m$ , corresponding to  $\Delta G_{\text{ps}} = \Delta G_{\text{mic}}(2) - \Delta G_{\text{mic}}(1)$ . Thus  $\Delta G_{\text{ps}}$  can be approximately used to compare the strengths of the interactions between SDS and perfumes. The obtained CMC and the derived thermodynamic parameters are shown in Table 3.

As clearly shown in Table 3, the effects of perfumes on the CMC values of SDS and the SDS/perfume interaction thermodynamic parameters are related to the molecular structures and the hydrophilicity/hydrophobicity degree of perfumes, i.e.,  $\log P$ . Generally, all these perfumes reduce the CMC of SDS and most of the perfumes in the intermediate  $\log P$  region show higher ability of reducing the CMC. That is because most of perfume molecules with intermediate  $\log P$  values penetrate into the palisade layer of the SDS micelles. In that case, they can take part in the formation of the SDS micelles and enhance the hydrophobic interaction among the SDS molecules. Comparing with  $\zeta$  potential, size and aggregation number, the CMC values do not vary in the same trend with the change of  $\log P$ , possibly because the CMC values reflect the ability of the micellization whereas the other three parameters are the properties of micelles above CMC. As to  $\Delta H_{\text{mic}}$ , the values with the perfumes in the lower  $\log P$  region ( $\log P < 2.0$ ) and some of the perfumes in the intermediate  $\log P$  region ( $2.0 < \log P < 3.5$ ) are more exothermic than that of SDS, whereas the  $\Delta H_{\text{mic}}$  values with the other perfumes do not have obvious difference from that of SDS.

Since  $\Delta G_{\text{mic}}$  and  $\Delta G_{\text{ps}}$  values are proportional to CMC values, the  $\Delta G_{\text{ps}}$  values for the SDS/perfume systems in the higher and lower  $\log P$  regions ( $\log P < 2.0$  and  $\log P > 3.5$ ) are almost close to zero. In contrast, the  $\Delta G_{\text{ps}}$  values with the perfumes in the intermediate  $\log P$  region are much more negative, although these data points do not change with  $\log P$  values monotonously. It is inferred that the binding of SDS with the perfumes in the intermediate  $\log P$  is more spontaneous than that in the other two  $\log P$  regions. This infers that the interactions of SDS with both the hydrophilic and hydrophobic moieties of the perfumes can contribute the self-assembly of the mixtures. Besides,  $\Delta S_{\text{mic}}$  is positive for all the perfumes and the contribution of the  $T\Delta S_{\text{mic}}$  values to  $\Delta G_{\text{mic}}$  are much larger than that of the  $\Delta H_{\text{mic}}$  values, which indicates the micellization of SDS with the perfumes is strongly driven by entropy. However, in the above effects of the perfumes on the CMC and their interaction with SDS ( $\Delta G_{\text{ps}}$ ), Menthyl Acetate and Methyl Paraben are two exceptions. These two perfumes not only significantly decrease the CMC of SDS, but also dramatically change the enthalpy of micellization. The  $\log P$  values of Menthyl Acetate and Methyl Paraben are 3.78 and 1.70, respectively, which are very close to the boundaries of the intermediate region of  $2.0 < \log P < 3.5$  we defined. Although the effects of these two perfumes on CMC and  $\Delta G_{\text{ps}}$  are consistent with the behaviour of the perfumes in the intermediate region of  $2.0 < \log P < 3.5$ , their effects on the  $\zeta$  potential and size of the SDS micelles are more consistent with the perfumes in the regions of  $\log P < 2.0$  or  $\log P > 3.5$ . So the present defined regions are kept.

Combining with all the above results, general trends for the effects of the perfumes on the micellization of SDS and localization of the perfume molecules in the micelles can be identified. (I) The perfumes in the low  $\log P$  region, i.e., more hydrophilic perfumes have a weak influence on the CMC of SDS and the molecular packing in the SDS micelles. These perfumes only partially incorporate into micelles and many free perfume molecules are left in the bulk solutions. Localization within the SDS micelle is predominantly in the headgroup regions. (II) The perfumes in the high  $\log P$  region swell the SDS micelles significantly but have little change in the CMC of SDS. The free Gibbs interaction energy of SDS with the perfumes in the high  $\log P$  region is similar to that in the

low  $\log P$  region. The perfumes in the high  $\log P$  region are more hydrophobic and thus their fraction of perfume molecules incorporated in micelles is higher and they are solubilized near the hydrophobic core region of the SDS micelles. (III) The most interesting but complicated region is certainly the intermediate  $\log P$  region. The penetration of the perfumes into the palisade layer of the SDS micelles results in the intermediate incorporated fraction and micelle growth, but more negative  $\Delta G_{\text{ps}}$  values reflect the stronger spontaneity of the SDS/perfume interaction in this region. The effects of the perfumes on the physicochemical properties of the SDS micelles do not always vary in the identical order of the  $\log P$  values, which suggests that the effects of perfumes on SDS micelles not only depend on the  $\log P$  values but also on other molecular structure factors, such as molecular conformation discussed above.

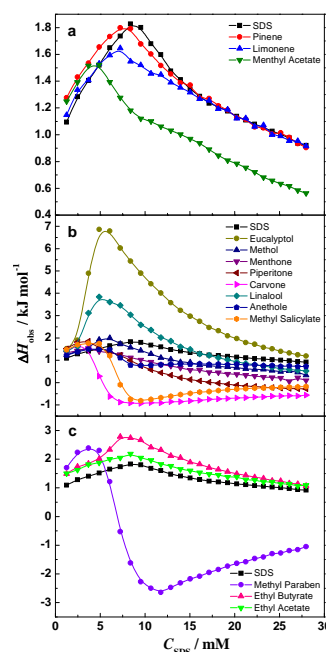


**Fig. 6.** ITC curves for titrating 200 mM SDS solution into water and 0.3 wt% perfume aqueous solution with (a)  $\log P > 3.5$ , (b)  $2.0 < \log P < 3.5$  and (c)  $\log P < 2.0$ .

**Table 3.** Critical micelle concentration and thermodynamic parameters for SDS in the absence and presence of perfumes at 25.00 °C.

Systems	CMC (mmol kg <sup>-1</sup> )	$\Delta G_{\text{mic}}$ (kJ mol <sup>-1</sup> )	$\Delta H_{\text{mic}}$ (kJ mol <sup>-1</sup> )	$\Delta S_{\text{mic}}$ (J mol <sup>-1</sup> K <sup>-1</sup> )	$\Delta G_{\text{ps}}$ (kJ mol <sup>-1</sup> )	
SDS	8.4	-21.9	-1.2	69.5		
$\log P > 3.5$	SDS/Pinene	7.8	-22.2	-1.2	70.6	-0.3
	SDS/Limonene	7.1	-22.7	-0.9	73.1	-0.8
	SDS/Menthyl Acetate	4.3	-25.0	-1.1	80.1	-3.1
	SDS/Eucalyptol	5.6	-23.8	-8.5	51.2	-1.9
$2.0 < \log P < 3.5$	SDS/Menthol	5.7	-23.7	-1.7	73.8	-1.8
	SDS/Menthone	3.7	-25.7	-1.7	80.4	-3.8
	SDS/Piperitone	3.2	-26.3	-2.1	81.3	-4.4
	SDS/Carvone	2.7	-27.1	-3.3	79.9	-5.2
	SDS/Linalool	5.3	-24.0	-6.6	58.4	-2.1
	SDS/Anethole	4.6	-24.7	-1.2	78.7	-2.8
	SDS/Methyl Salicylate	3.9	-25.4	-2.8	75.9	-3.5
	SDS/Methyl Paraben	3.8	-25.5	-6.1	65.2	-3.6
$\log P < 2.0$	SDS/Ethyl Butyrate	7.9	-22.2	-2.2	67.1	-0.3
	SDS/Ethyl Acetate	8.4	-21.9	-1.1	69.8	0.0

## Conclusion

This work has investigated the interaction of a large set of perfumes with SDS and the resulting effects on the SDS micelles. These perfumes have different hydrophilicity/hydrophobicity degrees and molecular conformation, so they show different impacts on the micellization of SDS and exhibit different partition and localization in the SDS micelles. The investigated perfume molecules can be classified into three different regions according to the  $\log P$  scale. Hydrophilic perfumes with  $\log P < 2.0$  partially incorporate into the SDS micelles and locate in the headgroup regions, so they almost do not change the size of the micelles. Very hydrophobic perfumes with  $\log P > 3.5$  are fully solubilized in the SDS micelles and locate near the core of micelle, causing significant micelle swelling. In the above two  $\log P$  regions, the hydrophilicity/hydrophobicity of the perfume molecules is crucial to determine the structure of the SDS micelles but has little effect on the CMC values. In other words, more hydrophobic perfumes induce larger SDS micelles with larger  $\zeta$  potential and larger aggregation number. In the intermediate  $\log P$  range ( $2.0 < \log P < 3.5$ ), the perfumes decrease the CMC of SDS more obviously and show more spontaneous interaction with SDS, and the  $\zeta$  potential, size and aggregation number of SDS/perfume mixed micelles increase with the increase of  $\log P$ , but the increasing extents are smaller than those in the range of  $\log P > 3.5$ . The fluctuated results may be attributed to the influence of other molecular structure factors besides the hydrophilicity/hydrophobicity degree. As a result, two different types of perfumes are identified in this region. One type of perfumes penetrate into the palisade layer of the SDS micelle, leading to the intermediate growth of the SDS micelles as well as  $\zeta$  potential and aggregation number, while another type of perfumes incorporate with the headgroup regions of the SDS micelles, similar to the perfumes in the low  $\log P$  region. In summary, the combination of the comprehensive results from  $\zeta$  potential, SAXS, one- and two-dimensional NMR and ITC provides more reliable understanding to the interaction between perfumes and surfactants, and more accurately estimation about the effects of the perfumes on surfactant micelles, which in turn may assist the design or improvement of formulations for home and personal care products.

## Acknowledgements

We are grateful for financial support from National Natural Science Foundation of China (Grants 21025313, 21321063) and Procter and Gamble Technology (Beijing) Co. Ltd. We also appreciate the BL16B1 beamline of Shanghai Synchrotron Radiation Facility (SSRF) for supporting the X-ray measurements (15ssrf02351) and this work benefitted from SasView software, originally developed by the DANSE project under NSF award DMR-0520547.

## Notes and references

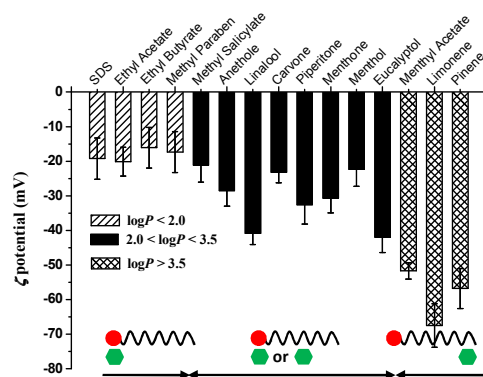
- J. Rao and D. J. McClements, *Food Hydrocolloid.*, 2012, 26, 268–276.
- J. Rao and D. J. McClements, *Food Chem.*, 2012, 134, 749–757.
- S. E. Friberg, *Adv. Colloid Interface Sci.*, 1998, 75, 181–214.
- P. Aikens and S. E. Friberg, *Curr. Opin. Colloid Interface Sci.*, 1996, 1, 672–676.
- S. Herman, *Cosmet. Toiletries*, 2006, 121, 59–67.
- J. M. Behan and K. D. Perring, *Int. J. Cosmet. Sci.*, 1987, 9, 261–268.
- S. E. Friberg, A. Al-Bawab, J. D. Sandberg, J. L. Barber, Q. Yin and P. A. Aikens, *J. Surfactants Deterg.*, 1999, 2, 159–165.
- Z. Zhang, S. E. Friberg and P. A. Aikens, *Int. J. Cosmet. Sci.*, 2000, 22, 181–199.
- N. W. Lloyd, E. Kardaras, S. E. Ebeler and S. R. Dungan, *J. Phys. Chem. B*, 2011, 115, 14484–14492.
- Z. Zhang, T. Denler and S. E. Friberg, *Int. J. Cosmet. Sci.*, 2000, 22, 105–119.
- Q. Qu, E. Tucker and S. D. Christian, *J. Incl. Phenom. Macrocycl. Chem.*, 2003, 45, 83–89.
- Y. Tokuoka, H. Uchiyama, M. Abe and S. D. Christian, *Langmuir*, 1995, 11, 725–729.
- Y. Tokuoka, H. Uchiyama and M. Abe, *J. Phys. Chem.*, 1994, 98, 6167–6171.
- Y. Tokuoka, H. Uchiyama, M. Abe and K. Ogino, *J. Colloid Interface Sci.*, 1992, 152, 402–409.
- R. Nagarajan, *Curr. Opin. Colloid Interface Sci.*, 1996, 1, 391–401.
- V. Suratkar and S. Mahapatra, *J. Colloid Interface Sci.*, 2000, 225, 32–38.
- E. Fischer, W. Fieber, C. Navarro, H. Sommer, D. Benczédi, M. Velazco and M. Schönhoff, *J. Surfactants Deterg.*, 2009, 12, 73–84.
- I. Kayali, K. Qamhieh and B. Lindman, *J. Dispersion Sci. Technol.*, 2006, 27, 1151–1155.
- R. Bradbury, J. Penfold, R. K. Thomas, I. Tucker, J. Petkov, C. Jones and I. Grillo, *Langmuir*, 2013, 29, 3234–3245.
- J. Penfold, I. Tucker, A. Green, D. Grainger, C. Jones, G. Ford, C. Roberts, J. Hubbard, J. Petkov, R. K. Thomas and I. Grillo, *Langmuir*, 2008, 24, 12209–12220.
- R. Bradbury, J. Penfold, R. K. Thomas, I. Tucker, J. Petkov and C. Jones, *Langmuir*, 2013, 29, 3361–3369.
- R. Bradbury, J. Penfold, R. K. Thomas, I. Tucker, J. Petkov and C. Jones, *J. Colloid Interface Sci.*, 2013, 403, 84–90.
- J. Penfold, E. Staples, I. Tucker, L. Soubiran, A. Khan Lodi, L. Thompson and R. K. Thomas, *Langmuir*, 1998, 14, 2139–2144.
- J. Penfold, E. Staples, I. Tucker, L. Soubiran and R. K. Thomas, *J. Colloid Interface Sci.*, 2002, 247, 397–403.
- Md. H. Uddin, N. Kanei and H. Kunieda, *Langmuir*, 2000, 16, 6891–6897.
- N. Lourith and M. Kanlayavattanakul, *Int. J. Cosmet. Sci.*, 2009, 31, 255–261.
- M. Corazza, M. M. Lauriola, M. Zappaterra, A. Bianchi and A. Virgili, *J. Eur. Acad. Dermatol.*, 2009, 24, 1–6.
- J. N. Labows, J. C. Brahm, and Cagan, R. H. In *Surfactants in Cosmetics. Surfactant Science Series*, ed. M. M. Rieger and L. D. Rhein, Marcel Dekker: New York, 1997, 68, pp. 605–619.
- F. Tian, X. Li, Y. Wang, C. Yang, P. Zhou, J. Lin, J. Zeng, C. Hong, W. Hua, X. Li, X. Miao, F. Bian and J. Wang, *Nucl. Sci. Tech.*, 2015, 26, 030101 1–6.
- SasView, <http://www.sasview.org/>
- Hammouda, B. *J. Res. Natl. Inst. Stan.*, 2013, 118, 1–24.
- W. Caetano, E. L. Gelamo, M. Tabak and R. Itri, *J. Colloid Interface Sci.*, 2002, 248, 149–157.
- R. Itri and L. Q. Amaral, *Phys. Rev. E*, 1993, 47, 2551–2557.
- Romani, A. P.; Gehlen, M. H.; Itri, R. *Langmuir*, 2005, 21, 127–133.
- L. J. Waters, T. Hussain and G. M. B. Parkes, *J. Chem. Thermodynamics*, 2012, 53, 36–41.
- K. Bouchemal, *Drug Discovery Today*, 2008, 13, 960–972.
- D. Kelley and D. J. McClements, *Food Hydrocolloid.*, 2003, 17, 73–85.
- Y. Li, P. Li, J. Wang, Y. L. Wang, H. Yan and R. K. Thomas, *Langmuir*, 2005, 21, 6703–6706.

- 39 D. Chu and J. K. Thomas, *J. Am. Chem. Soc.* 1986, 108, 6270–6276.
- 40 Y. L. Wang, B. Han, H. Yan and J. C. T. Kwak, *Langmuir*, 1997, 13, 3119–3123.
- 41 J. Lu, A. Marrocco, T. Su, R. K. Thomas and J. Penfold, *J. Colloid Interface Sci.*, 1993, 158, 303–316.

## Table of Contents

## Modulation of Partition and Localization of Perfume Molecules in Sodium Dodecyl Sulfate Micelles

Yaxun Fan,<sup>a</sup> Haiqiu Tang,<sup>\*b</sup> Ross Strand,<sup>b</sup> and Yilin Wang<sup>\*a</sup>



Relate aggregation behavior of surfactants to the corresponding structures of perfume molecules in terms of micellar structures, partitioning and localization of perfumes, and thermodynamic parameters of interaction process.